Research paper

Acta Neurobiol Exp 2017, 77: 1–17

ACTA NEUROBIOLOGIÆ EXPERIMENTALIS

Effects of epidural compression on stellate neurons and thalamocortical afferent fibers in the rat primary somatosensory cortex

Tzu-Yin Yeh[1], Guo-Fang Tseng[2,3], Chi-Yu Tseng[4], Yung-Hsin Huang[3], and Pei-Hsin Liu[1, 2, 3]*

[1] Institute of Medical Sciences, Tzu Chi University, Hualien, Taiwan, [2] Department of Anatomy, Tzu Chi University, Hualien, Taiwan, [3] Institute of Physiological and Anatomical Medicine, Tzu Chi University, Hualien, Taiwan, [4] Department of Neurology, Taichung Tzu Chi Hospital, Taichung, Taiwan,

** Email: peihsin@mail.tcu.edu.tw*

A number of neurological disorders such as epidural hematoma can cause compression of cerebral cortex. We here tested the hypothesis that sustained compression of primary somatosensory cortex may affect stellate neurons and thalamocortical afferent (TCA) fibers. A rat model with barrel cortex subjected to bead epidural compression was used. Golgi-Cox staining analyses showed the shrinkage of dendritic arbors and the stripping of dendritic spines of stellate neurons for at least 3 months post-lesion. Anterograde tracing analyses exhibited a progressive decline of TCA fiber density in barrel field for 6 months post-lesion. Due to the abrupt decrease of TCA fiber density at 3 days after compression, we further used electron microscopy to investigate the ultrastructure of TCA fibers at this time. Some TCA fiber terminal profiles with dissolved or darkened mitochondria and fewer synaptic vesicles were distorted and broken. Furthermore, the disruption of mitochondria and myelin sheath was observed in some myelinated TCA fibers. In addition, expressions of oxidative markers 3-nitrotyrosine and 4-hydroxynonenal were elevated in barrel field post-lesion. Treatment of antioxidant ascorbic acid or apocynin was able to reverse the increase of oxidative stress and the decline of TCA fiber density, rather than the shrinkage of dendrites and the stripping of dendritic spines of stellate neurons post-lesion. Together, these results indicate that sustained epidural compression of primary somatosensory cortex affects the TCA fibers and the dendrites of stellate neurons for a prolonged period. In addition, oxidative stress is responsible for the reduction of TCA fiber density in barrels rather than the shrinkage of dendrites and the stripping of dendritic spines of stellate neurons.

Key words: epidural compression, stellate neuron, thalamocortical afferent fiber, ascorbic acid, apocynin, somatosensory cortex

INTRODUCTION

A number of neurological disorders such as epidural or subdural hematoma, head trauma, intracerebral hemorrhage, brain tumor, localized brain edema, or hemangioma (Chen et al. 2003, DeAngelis 2001, Lin et al. 2010, Mayer and Rincon 2005, Watanabe et al. 2001) can cause compression of cerebral cortex, leading to various functional deficits including the sensorimotor aspect (Burnett et al. 2005, Kundrotiene et al. 2002, Lin et al. 2010, Martinez et al. 2011, Moreira et al. 2006, Yang et al. 2006). However, the underlying mechanism remains largely unknown.

Apart from perception of somatosensation, the somatosensory cortex is essential in sensory-motor coordination via direct or indirect connections with motor cortex, basal nuclei, cerebellum, and spinal cord (Ferezou et al. 2007, Johansson and Cole 1992). Furthermore, the somatosensory cortex is involved in physical and cognitive functions (Dobkin 1991, Gallace and Spence 2009). The rodent vibrissa somatosensation is transmitted through the principal sensory trigeminal nucleus and then the thalamic ventral posteromedial (VPM) nucleus which emits glutamatergic thalamocortical afferent (TCA) fibers terminating in layer IV stellate neurons of primary somatosensory cortex (Kharazia and Weinberg 1994). Notably, the stellate neurons form a series of barrels which correspond to topographic distribution of contralateral vibrissae (Welker and Woolsey 1974). Fluid-percussion injury of the rat parietal cortex has been shown to impair somatosensory electrophysiology, demonstrated by the decreases in slope and increases in latency of vibrissa-evoked field potentials at 3 days post-injury (Sanders et al. 2001). More recently, a suppression of thalamocortical oscillations was also

Received 29 June 2016, accepted 2 January 2017

Correspondence should be addressed to P.-H. Liu
Email: peihsin@mail.tcu.edu.tw

observed following a similar injury (Kao et al. 2012). These findings raise the possibility that compression of the somatosensory cortex may impair the structure of thalamocortical connections.

Oxidative stress has been shown to play a critical role in the pathophysiology of traumatic brain injury (TBI) (Marklund et al. 2001). Following cortical impact, the activity of nicotinamide adenine dinucleotide phosphate (NADPH) oxidase which is constitutively expressed in cortical neurons (Serrano et al. 2003) rapidly increases and its product superoxide (O_2^-) is accumulated (Zhang et al. 2012). Excess O_2^- can lead to tissue damage through promoting hydroxyl radical (OH^-) formation and through combining with nitric oxide (NO) to form a potent oxidant peroxynitrite ($ONOO^-$) (Afanas'ev 2007). These reactive oxygen species (ROS; e.g., O_2^- and OH^-) and reactive nitrogen species (RNS; e.g., NO and $ONOO^-$) can cause lipid peroxidation (Zhang et al. 1999), protein nitration (Beckman and Koppenol 1996), and DNA damage (Mendez et al. 2004). Our earlier study has shown that treatment of NADPH oxidase inhibitor apocynin or antioxidant ascorbic acid prevents the reduction of somatosensory evoked potential (SSEP) amplitude caused by sustained epidural compression (Lin et al. 2010). These results suggest that oxidative stress may be involved in the pathological alterations of somatosensory cortex caused by compression.

The objective of the current study was to directly investigate the effect of sustained epidural compression of primary somatosensory cortex on the underlying layer IV stellate neurons and TCA fibers. To evaluate the arrangement of stellate neurons, the area of individual barrel was measured. Furthermore, the dendritic arbor of stellate neurons and the distribution of TCA fibers in the barrel cortex were also analyzed. In addition, the ultrastructure of TCA fibers was examined under electron microscope. To assess the oxidative stress after compression, we examined the expressions of oxidative markers 3-nitrotyrosine (3-NT) for protein nitration and 4-hydroxynonenal (4-HNE) for lipid peroxidation. In addition, a short-term regimen of ascorbic acid or apocynin administration was employed to animals to determine the role of oxidative stress in the pathological alterations of somatosensory cortex caused by compression.

METHODS

All experiments were carried out in accordance with the National Institute of Health (NIH) Guide for the Care and Use of Laboratory Animals and the guidelines provided by the Institutional Animal Care and Use Committee of Tzu Chi University. Animals were housed under veterinarian assistance and kept in environmentally controlled animal facilities on a constant 12-h light/dark cycle, with access to food and water *ad libitum*. Adult male Sprague Dawley rats (n=142, 200–250 g; Charles River, BioLASCO) subjected to epidural compression were divided and allowed to survive for 1 day, 3 days, 1 week, 2 weeks, 3 months, and 6 months, respectively. Twenty-nine sham-operated and 8 normal rats were also included. Additional 50 rats received antioxidant or vehicle treatment (see below).

Epidural compression surgery

Hemispherical plastic beads (5 mm in diameter and 1.5 mm in thickness) were utilized to administer the compression of cerebral cortex. The surgical procedure has been previously described in detail (Chen et al. 2003, Lin et al. 2010). In brief, each animal was anesthetized with chloral hydrate (315 mg/kg intraperitoneally; Merck, Darmstadt, Germany) and the head was mounted in a stereotaxic frame (51,600, Stoelting, IL). The body temperature of animal was maintained between 36.5°C and 37.5°C. A craniectomy (an elliptical hole with short diameter 4 mm and long diameter 6 mm) was performed on the right cranial vault under a Zeiss surgical microscope (OPMI pico). The plastic bead with its flat surface facing up was slowly implanted in the epidural space and thus incidentally sealed the hole of skull. The coordinates of bead center was 0.84 mm posterior and 4.5 mm lateral to bregma, overlying the right primary somatosensory cortex (Lin et al. 2010). The contralateral (left) control side was sham-operated without bead implantation. The scalp was fastened with 6-0 sutures (Silkam, B/BRAUN, Tuttlingen, Germany) and then the animal was transferred to a heated cage to be monitored for full recovery from anesthesia. In normal animals, no craniectomy was performed. Sham-operated animals received similar anesthesia and craniectomy without bead implantation.

Drug treatment

The drug doses required to obtain a significant efficacy were determined as previously described (Lin et al. 2010). The animals (n=44) underwent intraperitoneal injections, starting immediately after epidural compression surgery, with ascorbic acid (500 mg/kg; Sigma, St. Louis, MO) or apocynin (50 mg/kg; Sigma) in 0.1 M phosphate-buffered saline (PBS), pH 7.4. The animals were allowed to survive for 1 week and received one injection every 24 h. Control animals (n=6) received the same surgery and the vehicle (PBS) injections.

Tissue preparation

Animals were deeply anesthetized and perfused transcardially with saline for 5 min followed by a fixative 4% paraformaldehyde in 0.1 M phosphate buffer (PB), pH 7.3, at room temperature for 30 min. The brains were removed, stored in the same fixative for 4 h, and then protected in 30% sucrose in 0.1 M PB at 4°C until they sank. For cytochrome oxidase reaction, the cerebral cortices were separated, pressed between two glass slides with glass capillary tubes as spacers (Wilson et al. 2000), and immersed in 30% sucrose in 0.1 M PB at 4°C for 48 h to facilitate the tangential cut. The cortical sheets were then frozen in Tissue-Tek O.C.T. embedding medium (Sakura Finetek, Torrance, CA) and cut into 40 µm-thick tangential sections on a LEICA cryostat (CM1850, Nussloch, Germany). For immunohistochemistry or illustration of thalamocortical afferent fibers, frozen brains were cut into 20 µm-thick coronal sections. All reacted sections were mounted onto gelatin-coated slides, coverslipped using Permount (Fisher, Fair Lawn, NJ), and inspected with a Zeiss Axioplan microscope. Images of reacted sections were acquired using a SPOT cooled CCD camera (Diagnostic, Sterling Heights, MI) combined with a SPOT software (VR 4.6.3.8).

Cytochrome oxidase reaction

Through mitochondrial cytochrome oxidase reaction, layer IV stellate neurons were observed to form a series of barrels (Lin et al. 2010). To investigate whether epidural compression affects the arrangement of stellate neurons in layer IV of barrel cortex, the tangential-sectional area of each individual barrel was analyzed. Two normal, 5 sham-operated, 25 compressed (5 for each time point) animals were processed for cytochrome oxidase reaction. The tangential sections of barrel cortices were incubated in a solution, 0.05% 3, 3'-diaminobenzidine tetrahydrochloride (DAB; Sigma), 4% sucrose (Sigma), and 0.02% cytochrome c (Sigma) in 0.1 M PBS, at 37°C for 1 h in the dark and then washed with cold 0.1 M PBS. To minimize the error introduced by the individual variability between animals, the area of barrel on the compressed side was compared to the area of the contralateral corresponding barrel of the same animal. Thus we calculated the area ratio as the area of the compressed barrel over that of the contralateral corresponding barrel in each animal and the barrel area ratio as the average of area ratios of the same animal group.

Immunohistochemistry

To detect the oxidative stress, 2 normal, 4 sham-operated, 4 compressed, 4 compressed and ascorbic acid-treated, 4 compressed and apocynin-treated, and 2 compressed and vehicle-treated animals were processed for immunohistochemistry. First, selective sections were quenched in 1% H_2O_2 for 1 h and then blocked with 10% normal goat serum (Vector, Burlingame, CA) for 1 h at room temperature. Subsequently, sections were incubated in a solution containing mouse anti-3-NT (1:500; Chemicon, Temecula, CA) or rabbit anti-4-HNE (1:2000; Calbiochem, La Jolla, CA) in 0.1 M PBS for 18 h at 4°C and then in biotinylated goat anti-mouse IgG (1:200; Vector) or goat anti-rabbit IgG (1:200; Vector) for 1 h at room temperature. After rinses in 0.1 M PBS, all sections were treated in avidin-biotin-horseradish peroxidase (HRP) reagent (1:100; Vector) and reacted with 0.05% DAB and 0.01% H_2O_2 in 0.05 M Tris buffer, pH 7.4. To eliminate the influence of the slight variability in immunohistochemical processing between sections or animals, the optical density (OD) of immunoreactivity on the compressed side was compared to that on the contralateral side of the same section. Thus, we calculated the OD ratio as the OD of immunoreactivity of the whole area of the compressed barrel cortex over that of the contralateral cortex in each section and the mean OD ratio was the average of OD ratios of the same animal group.

Golgi-Cox staining

To visualize the dendritic arbor of stellate neurons, 2 normal, 9 sham-operated, 54 compressed (9 for each time point), 9 compressed and ascorbic acid-treated, 9 compressed and apocynin-treated, and 2 compressed and vehicle-treated animals were processed for Golgi-Cox staining. Animals were deeply anesthetized and perfused transcardially with saline at room temperature for 5 min. Brains were dissected and stored in a Golgi-Cox solution, 1% $HgCl_2$ (Sigma), 1% $K_2Cr_2O_7$ (Sigma), and 1% K_2CrO_4 (Sigma), for 2 weeks in the dark at room temperature. Brains were then immersed in 30% sucrose in 0.1 M PB for 1 week at 4°C. Coronal sections were cut at 100 µm thickness on a vibratome (Series 1000, TPI, St. Louis, MO) and immersed in 25% ammonium hydroxide (Sigma). Sections were then dehydrated in ethanols, cleared in xylene, and coverslipped. Neurons for analyses were selected on the basis of their location in cortical layer IV and their morphology displaying radially oriented spiny dendrites. Images were captured using a Zeiss Axioplan microscope equipped with a SPOT cooled CCD camera. Reconstruction of each spiny stellate neuron was performed by tracing the neuronal soma and dendrites in successive coronal sections with a 40× (for dendritic arbor) or a 100× (for dendritic spines) Zeiss Plan-Neofluar objective and a Zeiss camera lucida drawing tube as previously described (Chen et al. 2003). Six neurons in each animal were analyzed. The soma size (soma area) of stellate neurons was measured in the focal

plane with largest soma diameter. The dendritic field span means the greatest length between the most distal ends of dendritic tips of a stellate neuron. Because the secondary dendritic segments of stellate neurons have the largest number and length relative to other order segments (Ballester-Rosado et al. 2016), 2 or 3 secondary segments of each neuron were selected for dendritic spine density analyses. To examine the complexity of dendritic processes as a function of distance from neuron soma center, the number of crossings that occur at each concentric 20 μm ring was counted (Scholl ring analysis).

Tracing of thalamocortical afferent fibers

To reveal the TCA fibers, which originate from the thalamic VPM nuclei, in the barrel cortices after epidural compression, anterograde tracing was performed on 2 normal, 9 sham-operated, 54 compressed (9 for each time point), 9 compressed and ascorbic acid-treated, 9 compressed and apocynin-treated, and 2 compressed and vehicle-treated animals. One week before sacrifice, animals were anesthetized for stereotaxic surgery. Following a craniectomy, two microinjections (1 μl each) of 5% anterograde tracer Biotinylated Dextran Amine (BDA; Vector) in 0.1 M PBS were applied, using a microliter syringe (87,900, Hamilton, Reno, NV), into the right thalamic VPM nucleus for 20 min (10 min per injection). The coordinates (for right injections, interaural 5.2 mm, lateral 3.2 mm, inferior 5.8 mm; interaural 5.2 mm, lateral 2.4 mm, inferior 6.6 mm) of injection sites were decided according to a stereotaxic atlas of the rat brain (Paxinos and Watson 2007). For each animal, another two microinjections were applied into the left thalamic VPM nucleus to serve as contralateral control.

Illustration of thalamocortical afferent fibers

One week after BDA injections, animals were sacrificed and their brain cryosections were processed to reveal the BDA-filled TCA fibers. Using DAB chromogen to stain the BDA-filled TCA fibers is a more widely-used method, whereas biotinylated tyramine staining method has been reported to enhance the BDA signal (Furuta et al. 2011). Thus, both methods were performed in the current study. First, sections were treated in 1% H_2O_2 in 0.1 M PB for 1 h to remove the endogenous peroxidase activity. After rinsing three times in 0.1 M PBS, the first series of sections (to stain the TCA fibers brown) were treated in avidin biotin-HRP reagent (1:100; Vector) in 0.1 M PBS at room temperature for 1 h and subsequently reacted in 0.05% DAB and 0.01% H_2O_2 in 0.05 M Tris buffer, pH 7.4. For the second series of sections (to stain the TCA fibers black), the biotinylated tyramine was made by adding 100 mg of Sulpho-NHS-LC-Biotin (Pierce, Rockford, IL) to 40 ml of 50 mM borate buffer (pH 8.0, Pierce) and then adding 15 mg of tyramine-HCl (Sigma). Sections were first incubated overnight in avidin biotin-HRP reagent (1:100; Vector) in 0.1 M PBS at room temperature. After rinses in 0.1 M PBS, sections were reacted with 2.5 μM biotinylated tyramine, 3 μg/ml glucose oxidase (Sigma), and 2 mg/ml glucose (Sigma) for 30 min. This was followed by incubation for 2 h in avidin biotin-HRP reagent (1:100; Vector) in 0.1 M PBS. Sections were then reacted with 0.05% DAB, 0.027% $NiCl_2$, and 0.01% H_2O_2 in 0.05 M Tris buffer, pH 7.4. To counterstain the neurons, both series of sections were subsequently treated in 10% normal goat serum in 0.1 M PBS for 1 h at room temperature. Following three rinses in 0.1 M PBS, sections were incubated in mouse anti-NeuN (1:400; Chemicon) in 0.1 M PBS for 18 h at 4°C. Sections were washed with three changes of 0.1 M PBS and incubated in biotinylated goat anti-mouse IgG (1:200; Vector) in 0.1 M PBS at room temperature for 1 h. After three rinses in 0.1 M PBS, the first series of sections were treated in avidin biotin-HRP reagent (1:100; Vector) in 0.1 M PBS at room temperature for 1 h and subsequently reacted in Vector SG substrate (to reveal the neuronal cell bodies in blue-gray), whereas the second series of sections were treated in avidin biotin-alkaline phosphatase (AP) reagent (1:100; Vector) in 0.1 M PBS at room temperature for 1 h and subsequently reacted in Vector Red substrate (to reveal the neuronal cell bodies in red). Six TCA fiber patchs in each animal were analyzed. We quantified the distribution of TCA fibers in the barrel field. The area ratio=the area occupied by TCA fibers in one barrel/the total area of the barrel. The R/L area ratio=the area ratios of right cortex/those of left cortex of the same animal. The TCA fiber density ratio=the average of all R/L area ratios of the same animal group. The brain sections containing the thalamic VPM nuclei were also stained and inspected to verify the success of injections.

Electron microscopy

To further investigate the ultrastructure of BDA-filled TCA fibers after epidural compression, 5 3-day-compressed and 2 sham-operated animals were processed for electron microscopy. The rats first received BDA injections as described above. Then 5 rats were subjected to epidural compression and 2 rats were sham-operated. One week after BDA injections, animals were deeply anesthetized and perfused transcardially with saline for 5 min followed by a fixative 4% paraformaldehyde and 2% glutaraldehyde (Sigma) in 0.1 M phosphate buffer (PB), pH 7.3, at room temperature for 30 min. The brains were removed and stored in 2.5% glutaraldehyde in 0.1 M cacodylate buffer. Coronal brain slices were cut at 200 μm thickness on a vibratome

and processed to reveal the BDA-filled TCA fibers using avidin biotin-HRP reagent and DAB as described above. The layer IV of barrel cortex containing the stained TCA fibers was cut to proper size under a Zeiss surgical microscope, fixed with 1% OsO_4 (Electron Microscopy Sciences, Hatfield, PA) in 0.1 M cacodylate buffer, stained *en bloc* with 2% uranyl acetate (Electron Microscopy Sciences), dehydrated through graded ethanol series, and embedded in Spurr's resin (Electron Microscopy Sciences). Serial ultrathin sections were cut on a LEICA EM UC6 ultramicrotome and collected on formvar-coated grids. Sections were then observed on a transmission electron microscope (H-7500, Hitachi, Tokyo, Japan) and digital images were taken.

Image and data analyses

All quantifications were done by an observer blinded to the treatment groups. In order to ensure valid comparison, both images of compressed and contralateral somatosensory cortices were acquired using the same brightness and exposure settings. Image-Pro Plus software (Media Cybernetics, Silver Spring, MD) was used to analyze the digital photographs and the tracings of reacted sections. All data were given as mean ± standard error of the mean (SEM). Unless particularly noted, the one-way Analysis of Variance (ANOVA) followed by Tukey *post hoc* test was applied for multiple comparisons. Statistical analyses were performed with Prism 4.03 software (GraphPad, San Diego, CA). Differences between data were considered statistically significant if $P<0.05$.

RESULTS

Area of barrel

A hallmark of the rodent primary somatosensory cortex is the layer IV cellular organization as barrels. To determine whether epidural compression affects the arrangement of stellate neurons in layer IV of barrel cortex, the tangential-sectional area of each individual barrel

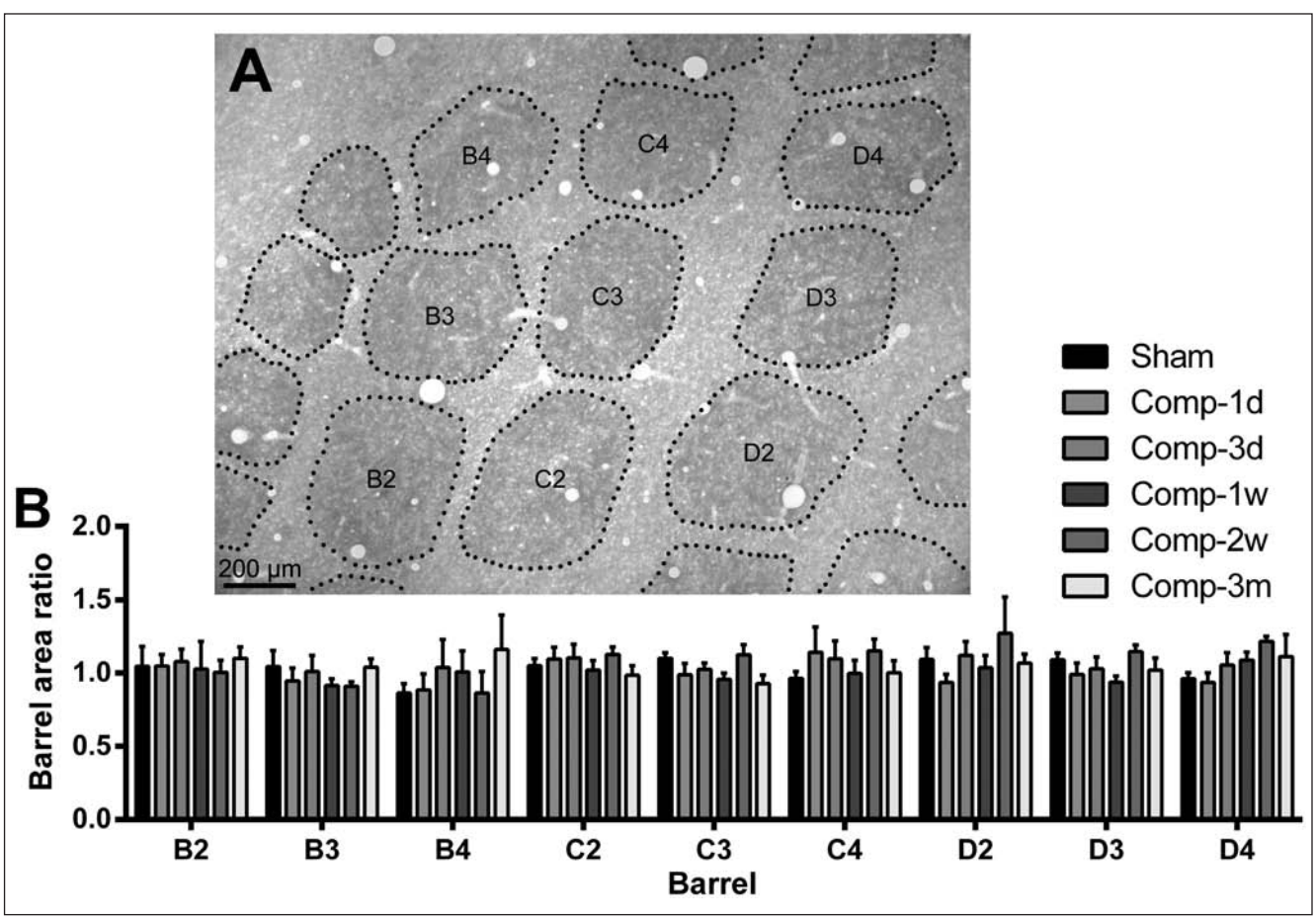

Fig. 1. Analyses of the areas of barrels in primary somatosensory cortex after epidural compression. (A) Revealed by cytochrome oxidase reaction, a representative photomicrograph shows the barrels in a tangential section through the cortical layer IV of a sham-operated rat. The center-located barrels B2–B4, C2–C4, and D2–D4 were analyzed. (B) The barrel area ratios. Abbreviations: d – day; w – week; m – month. Comp-1d means the animal group surviving for 1 day after compression. No statistical significance was detected.

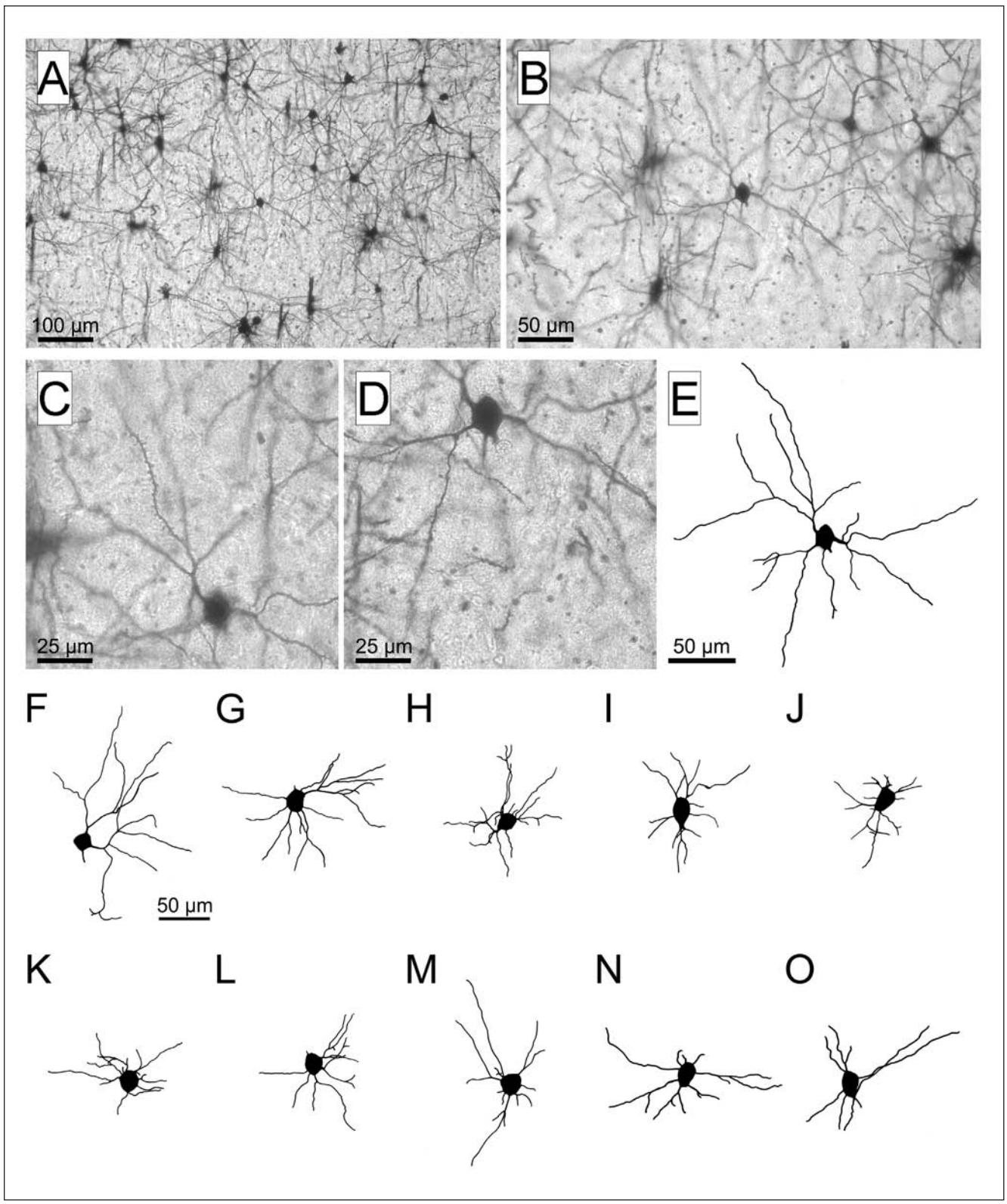

Fig. 2. Effects of epidural compression on the dendrites of stellate neurons in primary somatosensory cortices. (A) A representative photomicrograph shows the Golgi-Cox-stained neurons in a coronal section through the primary somatosensory cortex of a sham-operated animal. The neuron in the center of (A) was magnified in (B, C, and D) and traced in (E). Representative stellate neurons were illustrated from a sham-operated rat (F and G), rats which received epidural compression and survived for 1 day (H), 3 days (I), 1 week (J), 2 weeks (K), 3 months (L), and 6 months (M), and two rats which received epidural compression with ascorbic acid (N) and apocynin (O) treatment respectively and survived for 1 week. The scale bar in (F) is also for (G–O).

was analyzed. We selectively analyzed the center-located barrels B2–4, C2–4, and D2–4 (Fig. 1A) and found that there was no significant difference (P>0.05) between the barrel area ratios of the compressed animals and those of the sham-operated animals at any given time point (Fig. 1B). These results suggest that sustained epidural compression of barrel cortex did not alter the areas of barrels.

Dendrites of stellate neurons

To gain insight into the neuronal dendritic plasticity, the Golgi-Cox staining was performed. Spiny stellate neurons were identified on the basis of their location in cortical layer IV and their morphology displaying radially oriented spiny dendrites (Figs 2A–2E). The camera lucida drawings showed that compared to sham-operation (Figs 2F and 2G), there were substantial signs of shrinkage of neuronal dendritic arbors from 1 day to 3 months after compression (Figs 2H–2L). Nevertheless, the neuronal dendritic arbors at 6 months post-compression appeared to recover in comparison to those at 3 months (Figs 2L and 2M). In addition, treatment of ascorbic acid (Fig. 2N) or apocynin (Fig. 2O) for 1 week seemed likely to ameliorate the shrinkage of neuronal dendritic arbors (compared to Fig. 2J).

These pathological alterations were further quantified. We first analyzed the soma size (Fig. 3A), the total dendritic length (Figs 3B and 3C), the dendritic field span (Figs 3B and 3D), and the length of longest dendritic processes (Figs 3E and 3F). The soma size was not altered in 3 months but significantly increased at 6 months after compression (Fig. 3A). In contrast, sustained epidural compression rapidly attenuated the total dendritic length, the dendritic field span, and the length of longest dendritic process of stellate neurons to a lesser extent

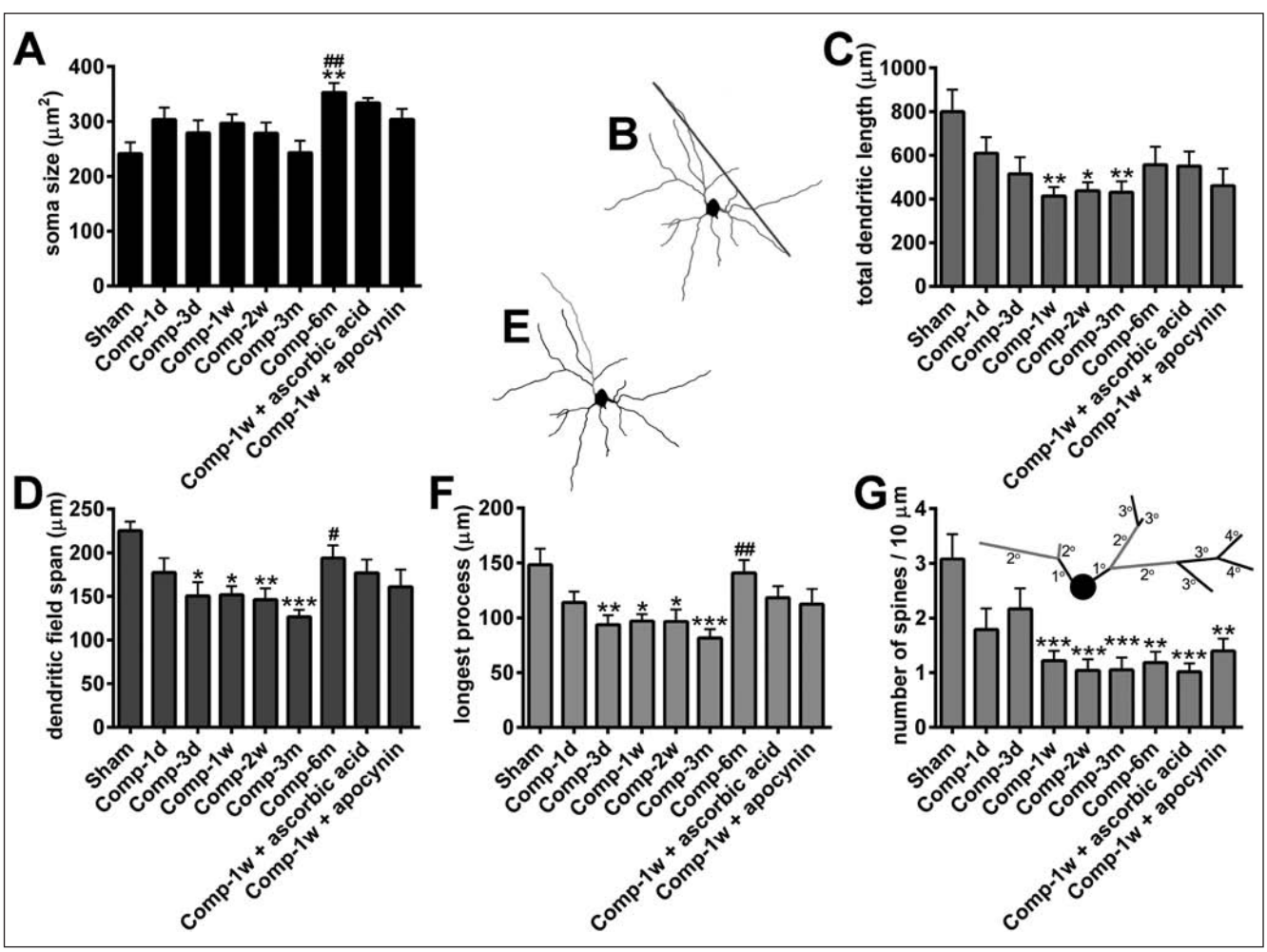

Fig. 3. Analyses of the somata and dendrites of stellate neurons in primary somatosensory cortices after epidural compression. (A–F) The soma size, the total dendritic length (red in B and C), dendritic field span (blue in B and D), and the length of longest dendritic process (green in E and F) are depicted in different colors for clarity. (G) The density of dendritic spines is the number of spines per 10 μm of the secondary (2°) dendritic segment. Mean ±SEM. Abbreviations: (d) day, (w) week, (m) month, *P<0.05, **P<0.01, ***P<0.001 *versus* the corresponding Sham group, #P<0.05, ##P<0.01 *versus* the corresponding animal group surviving for 3 months after compression (Comp-3m).

(Figs 3C, 3D, and 3F). The total dendritic length was significantly reduced by about 45–48% during 1 week to 3 months after compression (Fig. 3C). Furthermore, the stellate neurons in compressed barrel cortex had shorter dendritic field span (P<0.001) with a decrease of about 44% at 3 months after compression (Fig. 3D). When we focused on the length of longest process (Fig. 3F), there was also a striking difference (P<0.001) between the stellate neurons in 3 months-compressed cortices (reduced by 46%) and those in sham-operated cortices. These data indicate that sustained epidural compression led to a prolonged shrinkage of the dendritic arbors of stellate neurons for at least 3 months. Nevertheless, the dendritic field span (P<0.05) and the length of longest dendritic process (P<0.01) of stellate neurons recovered at 6 months in comparison

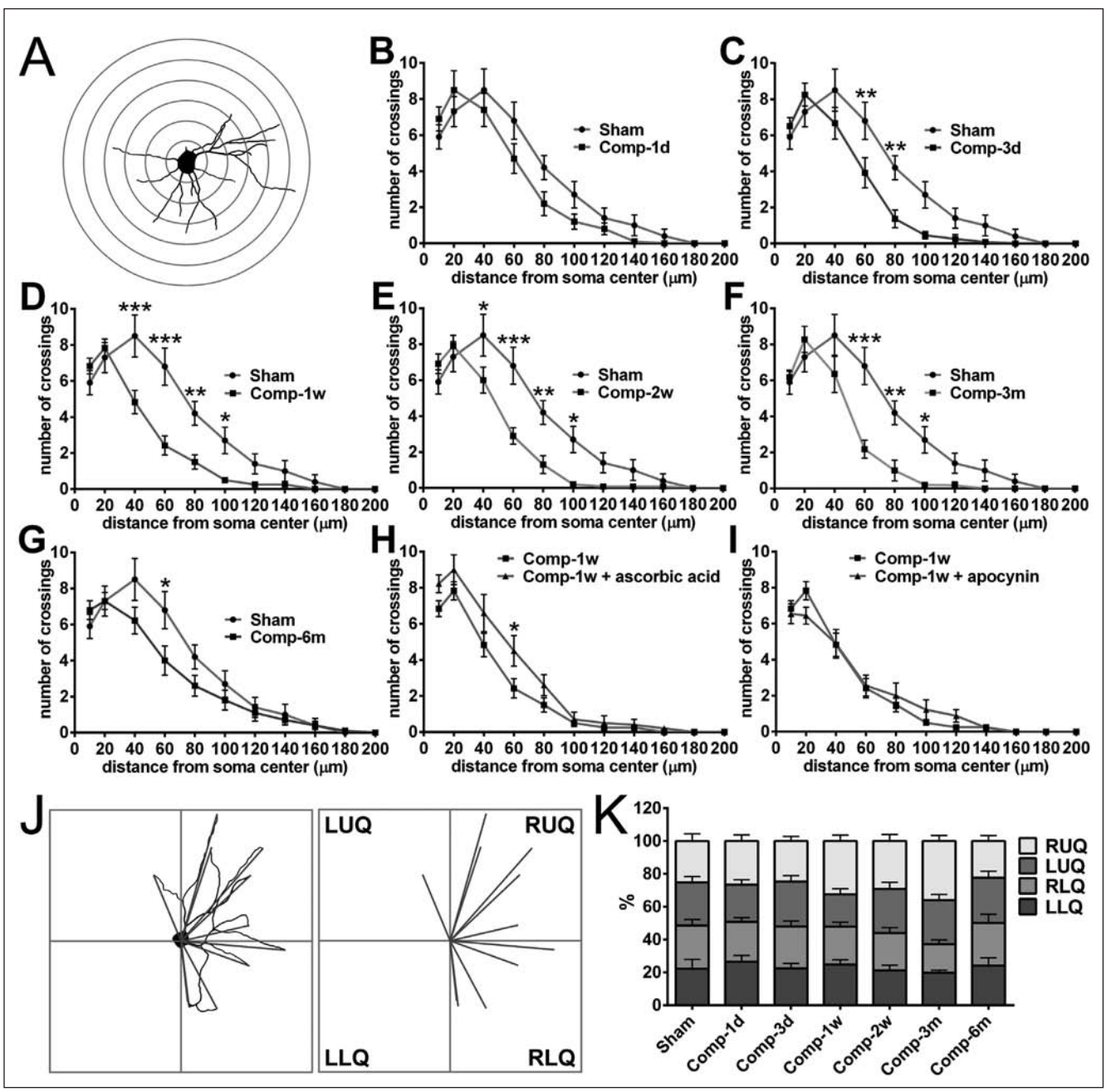

Fig. 4. The Scholl ring and dendritic orientation analyses of stellate neurons following epidural compression on primary somatosensory cortices. (A–I) Scholl ring analysis. Abbreviations: d – day, w – week, m – month, *P<0.05, **P<0.01, ***P<0.001 *versus* the corresponding number of crossings from another animal group, two-way ANOVA followed by Sidak *post hoc* test. (J) The dendritic orientation analysis. Abbreviations: (RUQ) right upper quadrant; (LUQ) left upper quadrant; (RLQ) right lower quadrant; (LLQ) left lower quadrant. (K) The number of lines in each quadrant was divided by the total number of lines in all four quadrants and expressed in percentage. No statistical significance was detected in dendritic orientation analyses.

to 3 months after compression (Figs 3D and 3F). Next, we further analyzed the density of dendritic spines (the number of spines per 10 μm of the secondary dendritic segment as depicted in Fig. 3G). We found that compared to sham-operation, sustained epidural compression significantly reduced the spine density starting at 1 week (Fig. 3G). On average the spiny stellate neurons in compressed cortices had a 66% decrease (P<0.001) in spine density on their secondary dendritic segments at 3 months post-compression. It is important to note that this decrease was not spontaneously reversed even at 6 months post-compression (Fig. 3G). We next examined whether antioxidants could alter the neuronal soma size or prevent the dendritic alterations caused by epidural compression. We found that treatment of ascorbic acid or apocynin for 1 week did not alter the soma size and failed to abolish the decreases of the total dendritic length, the dendritic field span, the length of longest dendritic process, and the dendritic spine density caused by sustained epidural compression (Figs 3A, 3C, 3D, 3F, and 3G, compared to Comp-1w). Together, these results suggest that treatment of ascorbic acid or apocynin was unable to prevent the shrinkage of dendritic arbors and stripping of dendritic spines of stellate neurons caused by sustained epidural compression.

To examine the complexity of dendritic processes as a function of distance from neuron soma center, the number of crossings that occur at each concentric 20 μm ring was counted for stellate neurons (Fig. 4A, Scholl ring analysis). We found that compared to sham-operation, the numbers of crossings occurring at the 60- to 80-μm distance from the soma center of stellate neurons were significantly reduced at 3 days (Fig. 4C, P<0.01) but not 1 day (Fig. 4B) after compression. At 1 and 2 weeks post-compression (Figs 4D and 4E), the decrease of crossings was found to occur at 40- to 100-μm, a wider range than that (60- to 80-μm) at 3 days. Nevertheless, the range gradually narrowed during 3 (60- to 100-μm) to 6 (60-μm) months post-compression (Figs 4F and 4G). In addition, the effect of antioxidants was also

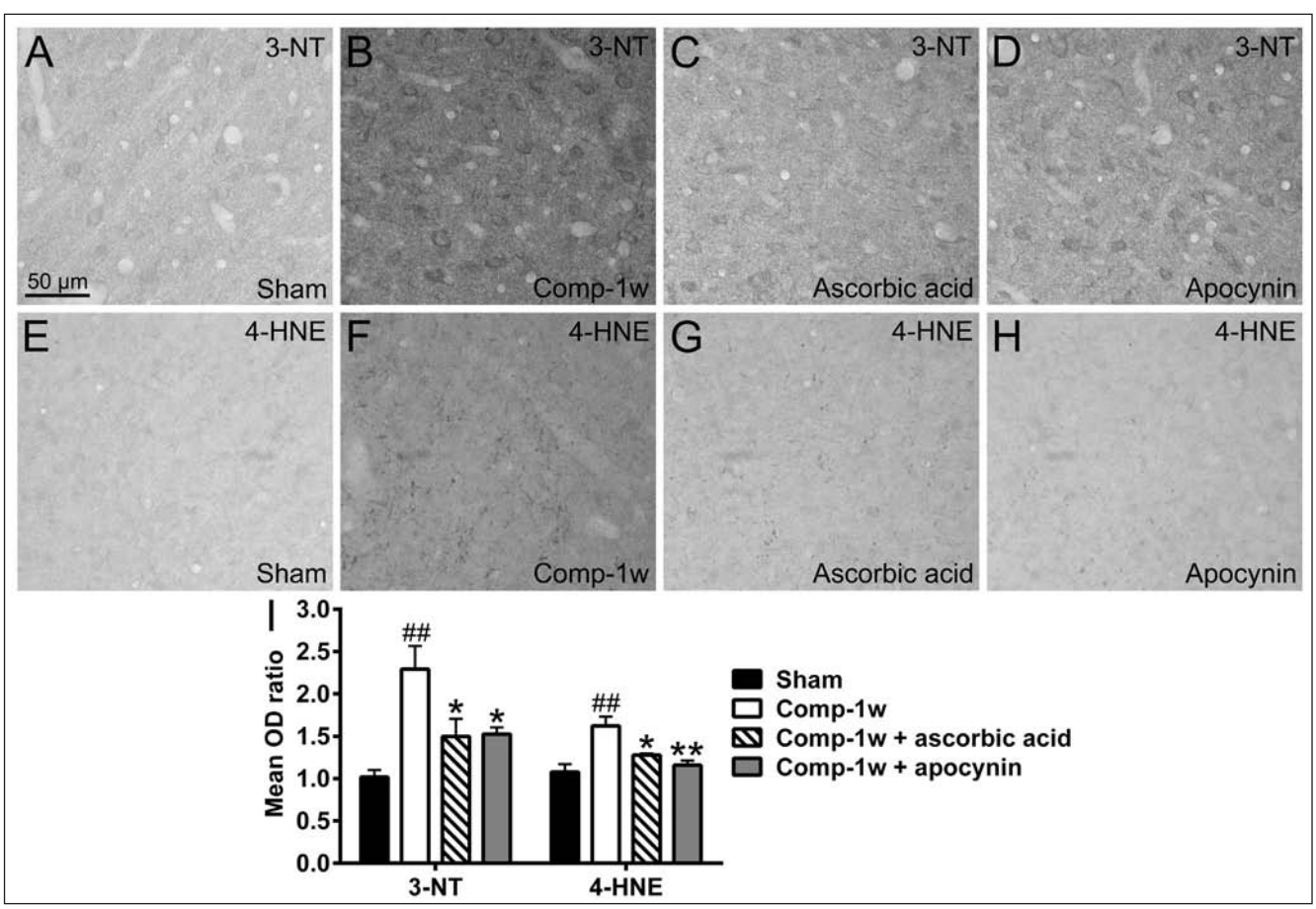

Fig. 5. The immunoreactivities of oxidative markers 3-NT and 4-HNE in layer IV of primary somatosensory cortex after epidural compression. Photomicrographs show the immunoreactivities of 3-NT (A–D) and 4-HNE (E–H) of a sham-operated (A and E), a compressed (B and F), a compressed and ascorbic acid-treated (C and G), and a compressed and apocynin-treated (D and H) animal. All animals survived for 1 week after surgery. The scale bar in (A) is also for (B–H). (I) Histograms show the mean optical density (OD) ratios of the immunoreactivities of 3-NT and 4-HNE. ##P<0.01 *versus* the corresponding Sham group, *P<0.05, **P<0.01 *versus* the corresponding animal group surviving for 1 week after compression (Comp-1w).

examined. Treatment of ascorbic acid for 1 week after compression only slightly elevated the number of crossings occurring at 60-μm (Fig. 4H) and treatment of apocynin had no effect (Fig. 4I). Together, these data indicate that the complexity of dendritic processes of stellate neurons was significantly reduced during 3 days to 6 months post-compression. Treatment of ascorbic acid or apocynin had little or no effect.

We next investigated the effect of epidural compression on the dendritic orientation of stellate neurons. The lines from the soma center to each end of dendritic tips of each individual stellate neuron were depicted (Fig. 4J, blue lines). With the cortical surface as a horizontal reference, the number of lines located within each of four quadrants was calculated. If a line was exactly located between two contiguous quadrants, 0.5 was assigned to each of the two quadrants. The number of lines in each quadrant was divided by the total number of lines in all four quadrants and expressed in percentage (Fig. 4K). There was no statistically significant difference between groups of animals, indicative of no conspicuous dendritic orientation bias in stellate neurons after epidural compression.

Expressions of oxidative markers

We next assessed the oxidative stress in the barrel field after epidural compression. Considering that the greatest alterations of neuronal dendrites and dendritic spines were seen starting from 1 week after compression (Figs 3 and 4), we examined the expressions of oxidative markers at 1 week rather than later time points to reduce the suffering of animals. Compared to sham-operation (Figs 5A and 5E), sustained epidural compression for 1 week remarkably increased both 3-NT and 4-HNE expressions by approximately 125% and 51%, respectively ($P<0.01$) in the barrel field (Figs 5B, 5F, and 5I). Notably, there is also an increase of 3-NT and 4-HNE expressions at 1 day post-compression as shown previously (Lin et al. 2010). We further examined whether antioxidants could block the oxidative stress caused by epidural compression. We found that treatment of ascorbic acid or apocynin for 1 week significantly suppressed the increases of 3-NT and 4-HNE (Figs 5B–5D and 5F–5I). Together, these data indicate that sustained epidural compression enhanced oxidative stress for at least 1 week in the underlying somatosensory cortex. Treatment of ascorbic acid or apocynin can prohibit the increase of oxidative stress.

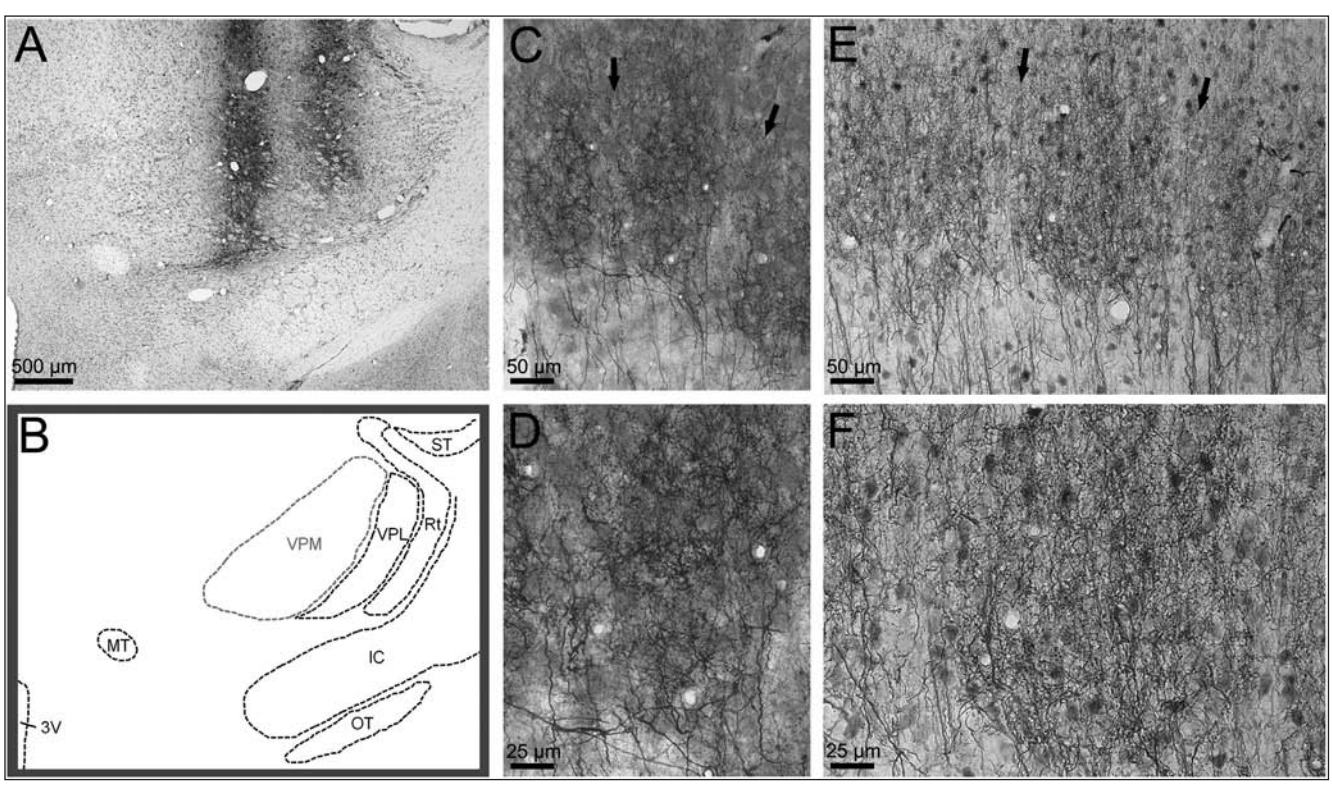

Fig. 6. The anterograde tracing of the thalamocortical afferent (TCA) fibers. The anterograde tracer BDA was applied into the ventral posteromedial (VPM) nucleus of right thalamus through two microinjections. (A) Two needle tracks (brown) in the injection site are evident in contrast to the Nissl counterstain using cresyl violet. The structures in (A) are illustrated in (B) for easy identification. Structures: (VPL) thalamic ventral posterolateral nucleus; (Rt) thalamic reticular nucleus; (ST) stria terminalis; (IC) internal capsule; (OT) optic tract; (MT) mammillothalamic tract; (3V) third ventricle. (C) The biotinylated tyramine staining method reveals the TCA fiber patchs in black (magnified in D) in contrast to the anti-NeuN counterstain (red) in a coronal section from a sham-operated rat. (E) The DAB chromogen reveals the TCA fiber patchs in brown (magnified in F) in contrast to the anti-NeuN counterstain (blue-gray). (C and E) The arrows indicate the septums between neighboring barrels.

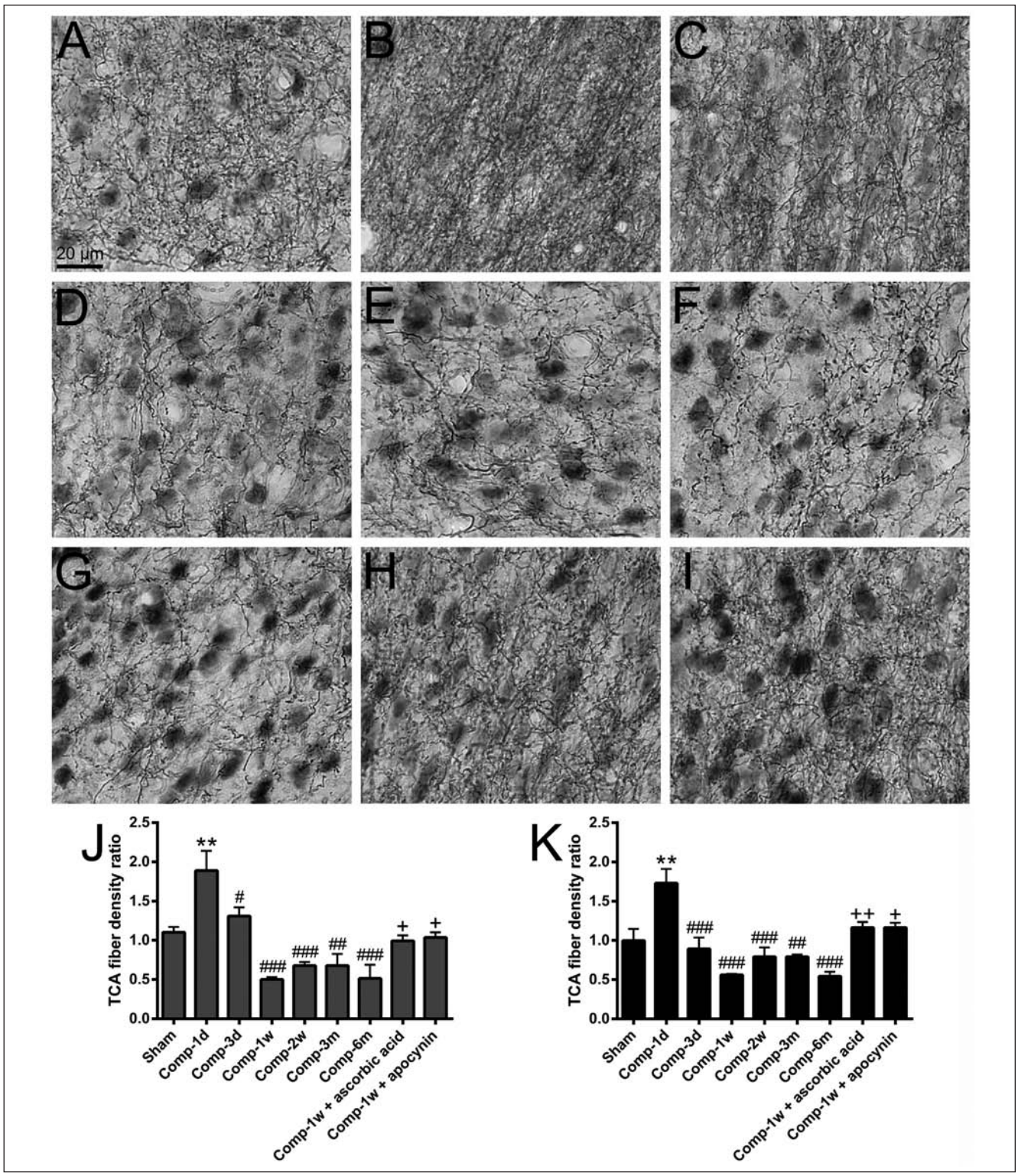

Fig. 7. The distribution of thalamocortical afferent (TCA) fibers in the barrels after epidural compression. (A–I) Micrographs show the BDA-filled TCA fibers (brown) in layer IV of right primary somatosensory cortices of a sham-operated rat (A), rats which received epidural compression and survived for 1 day (B), 3 days (C), 1 week (D), 2 weeks (E), 3 months (F), and 6 months (G), and two rats which received compression with ascorbic acid (H) and apocynin (I) treatment respectively and survived for 1 week. The TCA fiber density ratios in (J) were obtained from the data of a series of sections processed as shown in Figs 6E, F, and 7A–I, whereas those in (K) were obtained from the data of another series of sections processed as shown in Figs 6C and 6D. Abbreviations: d – day, w – week, m – month, ***P*<0.01 *versus* the corresponding Sham group, #*P*<0.05, ##*P*<0.01, ###*P*<0.001 *versus* the corresponding animal group surviving for 1 day after compression (Comp-1d), +*P*<0.05, ++*P*<0.01 *versus* the corresponding Comp-1w.

Thalamocortical afferent fibers

To investigate the distribution of TCA fibers in the barrel field, the anterograde tracer was applied into the thalamic VPM nucleus (Figs 6A and 6B). In one series of sections, the TCA fibers were stained black and the neuronal cell bodies were stained red (Figs 6C and 6D). In another series of sections, the TCA fibers were stained brown and the neuronal cell bodies were stained blue-gray (Figs 6E and 6F). In sham-operated animals, the elaborate TCA fibers were distributed within individual barrels, appearing as patches (Figs 6C–6F). Between the TCA fiber patches were septums (Figs 6C and 6E, arrows). We analyzed the TCA fiber density in individual barrels and found that compared to

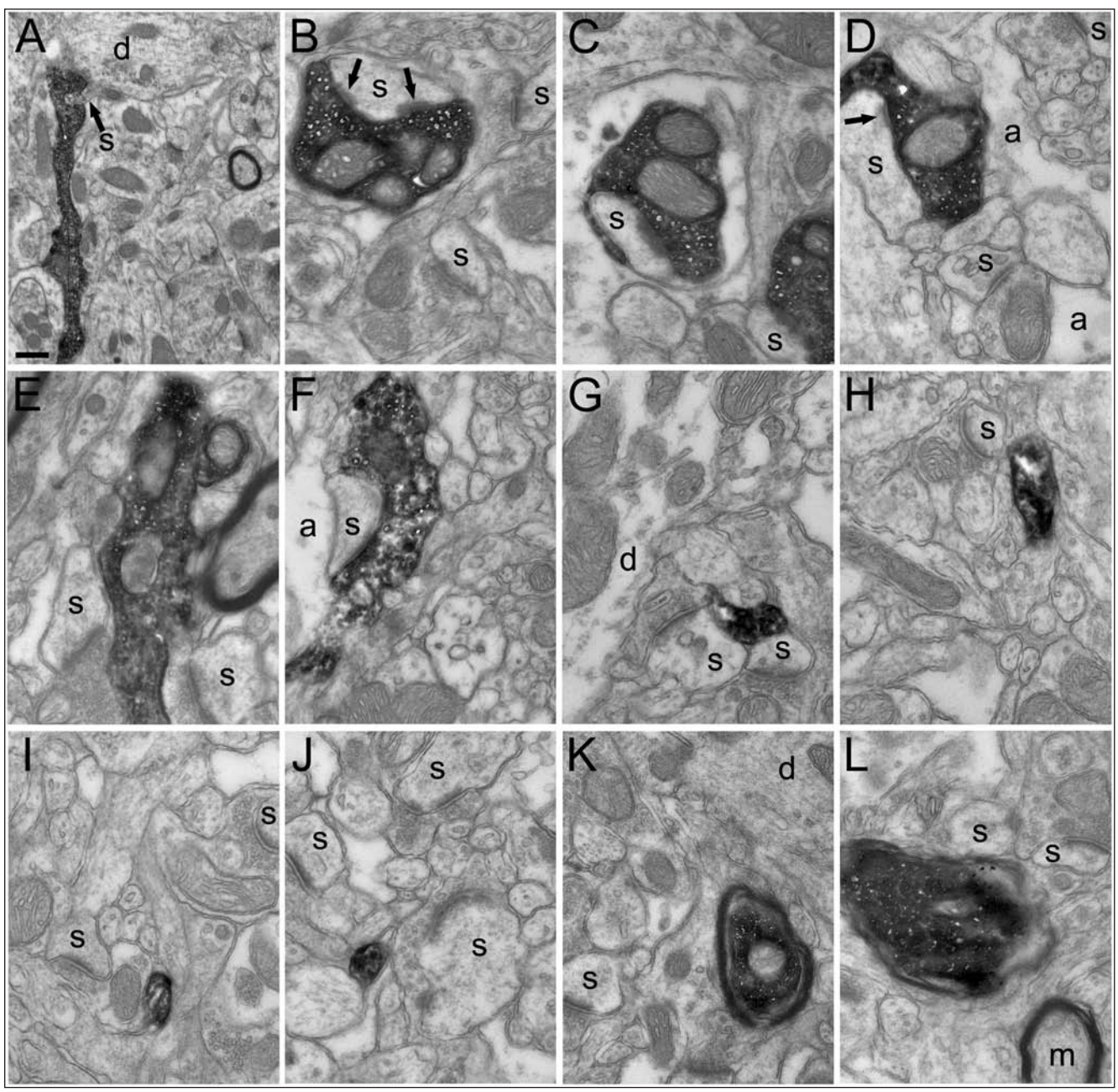

Fig. 8. The ultrastructure of thalamocortical afferent (TCA) fibers in the layer IV of barrel cortex at 3 days after epidural compression. (A) An electron micrograph shows a BDA-filled TCA fiber ending on a spine (s) of a dendrite (d) in a sham-operated rat. (B–D) Three BDA-filled TCA fiber terminals contained mitochondria and synaptic vesicles and ended by means of synaptic contacts (arrows) on dendritic spines (s) at 3 days after compression. Some small astrocytic processes (a) and dendritic spines in contact with unlabeled axon terminals were also seen in the vicinity. (E and F) Two BDA-filled terminals containing damaged mitochondria and fewer synaptic vesicles were distorted and broken. (G–J) The mitochondria and synaptic vesicles disappeared from four shrunken BDA-filled terminals. (K) A BDA-filled myelinated axon contained a dissolved mitochondrion. (L) The myelin sheath and mitochondria of a BDA-filled axon was disrupted at 3 days after compression. A myelinated axon (m) was also seen in the vicinity. Scale bar=600 nm for A and 200 nm for B–L.

the sham group, the TCA fiber density abruptly increased at 1 day post-compression, irrespective of the staining method (Figs 7A, 7B, 7J, and 7K). The rapid increase of TCA fiber density is likely due to the abrupt decrease of cortical layer thickness caused by epidural compression as shown in previous studies (Chen et al. 2003, Lin et al. 2010) and the little if any loss of TCA fibers at this time point. However, it is noteworthy that compared to the findings at 1 day post-compression (Fig. 7B), the TCA fiber density ratios progressively declined during 3 days (by approximately 48%) to 1 week (by approximately 68%) post-compression (Figs 7C, 7D, 7J, and 7K) and then maintained at a low level during 2 weeks to 6 months (Figs 7E–7G, 7J, and 7K).

Due to the abrupt decrease of TCA fiber density at 3 days after compression, we further used electron microscopy to investigate the ultrastructure of TCA fibers at this time (Fig. 8). The BDA-filled TCA fibers and their terminals were markedly electron dense under the electron microscope (Fig. 8A). At 3 days after compression, there were still a lot of BDA-filled TCA fiber terminals which contained several mitochondria and numerous synaptic vesicles and ended by means of synaptic contacts on dendritic spines (Figs 8B–8D). However, some BDA-filled axon terminal profiles with dissolved or darkened mitochondria and fewer synaptic vesicles were distorted and broken (Figs 8E and 8F). In many shrunken axon terminals, mitochondria and synaptic vesicles were absent (Figs 8G–8J). Furthermore, the disruption of mitochondria and myelin sheath was observed in some BDA-filled myelinated axons (Figs 8K and 8L).

We further tested the importance of ROS-mediated oxidative stress in the epidural compression-induced reduction of TCA fibers in the barrel cortex. Treatment with ascorbic acid or apocynin for 1 week (Figs 7H and 7I, compared to Fig. 7D) significantly improved the drastic reduction of TCA fiber density ratios caused by epidural compression (Figs 7J and 7K). Together, these data demonstrate that sustained epidural compression caused the reduction of TCA fibers in the barrel field and treatment of ascorbic acid or apocynin could partially prevent this pathological alteration.

DISCUSSION

In prior animal studies, TBI has been elicited by transient fluid percussion (Conti et al. 1998, Kao et al. 2012, Sanders et al. 2001, Sato et al. 2001) or impactor contusion (Grossman and Stein 2000, Kuypers and Hoane 2010, Matthews et al. 1998). Furthermore, short-lasting compression (<2 hours) has been applied on the cerebral cortices of animals using Plexiglas piston, brass or plastic cylinder (Burnett et al. 2005, Kundrotiene et al. 2002, Watanabe et al. 2001). In these studies, the tools used to cause injury could be exerted on the cerebral cortex in a relatively short period. On the contrary, the bead used in the present study allowed us to perform long-term and persistent compression of the cerebral cortices when the animals were moving freely in the cage. Thus, the present study could unveil for the first time the detailed alterations in the dendritic arbors of spiny stellate neurons and the distribution of TCA fibers in response to long-term and sustained epidural compression. In contrast to the cerebral ischemia (Burnett et al. 2005, Kundrotiene et al. 2002, Watanabe et al. 2001) and considerable cell death (Conti et al. 1998, Sato et al. 2001) observed in the prior TBI or short-lasting compression studies, sustained epidural compression performed here did not cause such intense pathological events (Chen et al. 2003, Lin et al. 2010). The diameter of cortical microvessels is only transiently and slightly reduced (Lin et al. 2010). Brain edema (Lin et al. 2010) and microglial activation (Chen et al. 2003) were not seen after epidural compression. Thus, our current study could focus on the plasticity of stellate neurons and TCA fibers in response to only physical compression which was not complicated with ischemia, cell death, brain edema, or microglial activation.

Another technical issue could be considered. The contralateral (left) side of animals was sham-operated without bead implantation and served as the contralateral control in the present study. As shown in our previous study (Lin et al. 2010), the barrels in the contralateral cortex are not deformed. The microvessels and the blood-brain barrier in the contralateral cortex are not damaged. The water content of both the compressed (right) and the contralateral cortices is maintained at the normal level, indicative of no edema occurring. These results suggest that there is not a general compression of the whole brain after unilateral epidural compression. Furthermore, the callosal connections between right and left primary somatosensory cortices mainly link the jaw representations (Hayama and Ogawa 1997). There is little if any connection between right and left barrels in the whisker representations. Thus, the effect of callosal connection on the contralateral barrel cortex after unilateral epidural compression is greatly reduced. In addition, the results of the contralateral cortices of the experimental animal group were not significantly different from those of the normal and the sham-operated groups in the current study. Taken together, all the above results strongly support that the contralateral (left) cortex is nearly unaffected by the compression of the right cortex.

In the present study, sustained epidural compression did not alter the areas of barrels, suggesting that under moderate compression, the stellate neurons of a barrel were still confined within the original horizontal field, even though the vertical depth of cortical layers was compressed (Chen et al. 2003, Lin et al. 2010). As a result, the stellate neurons would be in a more compact space under the

sustained epidural compression. Indeed, the density of layer IV neurons was increased following epidural compression (Chen et al. 2003). Collectively, these findings suggest that sustained epidural compression results in a smaller space for the underlying stellate neurons and may thus lead to the plasticity of their dendrites and afferent fibers.

Our current study is the first to demonstrate the reduction of TCA fibers in barrels for at least 6 months as a result of sustained epidural compression. Several lines of clinical and experimental investigations have shown that traumatic head injury often triggers secondary axonal injury, leading to neurological deficits. For example, multifocal axonal injury has been demonstrated in all five investigated patients with concussive head injury (Blumbergs et al. 1994). Furthermore, using electron microscopy, the degeneration of myelinated axons and presynaptic endings was observed in cortical biopsies of all eight investigated patients suffering head trauma complicated with epidural or subdural hematoma (Castejon 1998). In animal studies, fluid-percussion brain injury has been shown to cause widespread progressive axonal damage (Rodriguez-Paez et al. 2005). Moreover, the neuronal cell bodies directly under brain trauma are well-preserved but surrounded by massive degenerating axons (Matthews et al. 1998), suggesting that the intact neurons are stripped of their afferent fibers. These results together support the notion that neuronal axons are likely more susceptible to traumatic brain damage than neuronal cell bodies. A number of studies have established the critical role of oxidative stress in the TBI-induced axonal degeneration. TBI can elicit a depletion of antioxidant enzymes (Ansari et al. 2008) and an elevation of ROS-mediated oxidative stress in animals (Marklund et al. 2001, Pratico et al. 2002, Zhang et al. 1999) or humans (Paolin et al. 2002). The oxidative stress can cause a substantial loss of neuritic mitochondria and then a neurite retraction (de la Monte et al. 2000). In addition, the TBI-induced oxidative stress can reduce the levels of brain-derived neurotrophic factor (BDNF) and synaptic protein which are required for maintaining synaptic contacts and function (Ansari et al. 2008, Wu et al. 2006). It is also noteworthy that the TBI-induced oxidative stress can aggravate the increase of axolemmal permeability, leading to compaction of axonal neurofilament, reduction in microtubule density, and degradation of subaxolemmal spectrin (Buki et al. 1999, Lewen and Hillered 1998, Pettus and Povlishock 1996). These observations together corroborate that oxidative stress is tightly linked to TBI-caused secondary axonal injury. In our current study, treatment of apocynin (the NADPH oxidase inhibitor) or ascorbic acid (a potent ROS scavenger) significantly mitigated the compression-induced reduction of TCA fibers in barrels. It has been proposed that NADPH oxidase is expressed not only in microglia (Shimohama et al. 2000) but also in neurons and astrocytes (Noh and Koh 2000, Tammariello et al. 2000). This has led to the suggestion that treatment of apocynin in the present study may prohibit the overproduction of superoxide by neuronal or glial NADPH oxidase and then prevent the synaptic disconnection and the axonal cytoskeleton disruption. Another antioxidant ascorbic acid that we used here is, under physiological condition, highly concentrated in the brain and predominantly expressed in neurons (Grünewald 1993, Rice and Russo-Menna 1998). However, the endogenous ascorbic acid has been shown to be rapidly depleted after brain trauma, resulting in a massive production of ascorbic acid radicals (Awasthi et al. 1997, Tyurin et al. 2000). These findings suggest the essential role of ascorbic acid in the primary protection of brain against the brain trauma-induced oxidative stress. Taken together, all the above results and considerations provide strong supporting evidence that supplement of ascorbic acid or apocynin is able to counteract the oxidative stress and consequently prevent the reduction of TCA fiber density in the barrel field in our compression model.

Previous clinical and experimental studies have shown that neuronal dendrites and dendritic spines are also susceptible to TBI. As demonstrated in patients, head trauma complicated with epidural or subdural hematoma was observed to cause the degeneration of neuronal dendrites (Castejon 1998). Recently, animal studies in TBI also revealed a reduction in dendrites and dendritic spines of cortical neurons (Gao and Chen 2011, Winston et al. 2013). Furthermore, in our sustained epidural compression model, the total dendritic length and dendritic spine density of cortical layer III and V pyramidal neurons decrease immediately after compression (Chen et al. 2010b) and maintained at a low level for 1 year (Chen et al. 2003). With regard to layer IV stellate neurons, the current study demonstrates for the first time that their total dendritic length and dendritic spine density were significantly reduced from 1 week to 3 and 6 months respectively after compression. The molecular mechanisms underlying the withdrawal of dendrites and the stripping of dendritic spines have been investigated. TBI has been shown to elicit a loss of microtubule-associated protein 2 (MAP2) and neurofilament proteins in the dendrites of cortical neurons, leading to an impairment of dendritic arborization (Posmantur et al. 1996, 2000, Saatman et al. 1998). In line with these results, sustained epidural compression enhances the phosphorylation of MAP2 and tau (Chen et al. 2010a), resulting in the destabilization of microtubules and in turn the reconfiguration of dendrites. Moreover, sustained epidural compression triggers the *N*-methyl-D-aspartate (NMDA) receptor-mediated depolymerization of actin in the dendritic spines (Chen et al. 2015). This is also supported by evidences that blockade of NMDA receptor reverses the elimination of dendritic spines (Halpain et al. 1998, Vlachos et al. 2013, Zuo et al. 2005). Collectively, these

results suggest that sustained epidural compression may also act through the breakdown of microtubules and actin filaments to disrupt the dendrites and dendritic spines of layer IV stellate neurons. In addition, our current study showed that treatment of ascorbic acid or apocynin did not significantly rescue the epidural compression-induced reduction of the dendritic length, dendritic field span, and dendritic spine density of stellate neurons. These results strongly support that ROS-mediated oxidative stress is more associated with the reduction of TCA fibers in barrels rather than the shrinkage of dendrites and the stripping of dendritic spines of stellate neurons caused by sustained epidural compression.

The behavioral tests of rats subjected to epidural compression have been performed previously (Yang et al. 2006). The forelimb-use asymmetry test showed a long-term (1 month, the longest test time) motor deficit, whereas both the somatosensory asymmetry test and the vibrissae-evoked forelimb placing test revealed a short-term (several days) sensory deficit. Likewise, our previous study using the von Frey behavioral test and the electrophysiological method also demonstrated a sensory impairment seen only in the initial several days after compression (Lin et al. 2010). After that, the sensory impairment spontaneously recovered (Lin et al. 2010) although there is concomitantly a structural disruption of thalamocortical connections demonstrated in the current study. A possible explanation is the homeostatic synaptic response (Turrigiano 2012, Vlachos et al. 2013). The intact excitatory synapses may be strengthened and/or the inhibitory synapses may be weakened to compensate the loss of synapses caused by compression. However, as mentioned above, the somatosensory cortex is essential in sensory-motor coordination via direct or indirect connections with motor cortex, basal nuclei, cerebellum, and spinal cord (Ferezou et al. 2007, Johansson and Cole 1992), and is involved in physical and cognitive functions (Dobkin 1991, Gallace and Spence 2009). Thus, whether these higher-order coordinated functions are affected needs to be further investigated.

CONCLUSIONS

The present study provides direct evidence that sustained epidural compression of primary somatosensory cortex affects the TCA fibers and the dendrites of stellate neurons for a prolonged period. ROS-mediated oxidative stress is responsible for the reduction of TCA fibers in barrels rather than the shrinkage of dendrites and the stripping of dendritic spines of stellate neurons. Treatment of ascorbic acid or apocynin may be potentially an effective therapy for patients with cortical compression complicated by axonal disruption.

ACKNOWLEDGEMENTS

We thank the Electron Microscopy Laboratory of Tzu Chi University for technical assistance. This work was supported by a grant from the National Science Council of Taiwan (NSC 102-2320-B-320-002) and a grant from Tzu Chi University (TCIRP 101004-03) to Pei-Hsin Liu.

REFERENCES

Afanas'ev IB (2007) Signaling functions of free radicals superoxide & nitric oxide under physiological & pathological conditions. Mol Biotechnol 37: 2–4.

Ansari MA, Roberts KN, Scheff SW (2008) A time course of contusion-induced oxidative stress and synaptic proteins in cortex in a rat model of TBI. J Neurotrauma 25: 513–526.

Awasthi D, Church DF, Torbati D, Carey ME, Pryor WA (1997) Oxidative stress following traumatic brain injury in rats. Surg Neurol 47: 575–581.

Ballester-Rosado CJ, Sun H, Huang JY, Lu HC (2016) mGluR5 exerts cell-autonomous influences on the functional and anatomical development of layer IV cortical neurons in the mouse primary somatosensory cortex. J Neurosci 36: 8802–8814.

Beckman JS, Koppenol WH (1996) Nitric oxide, superoxide, and peroxynitrite: the good, the bad, and ugly. Am J Physiol 271: C1424–C1437.

Blumbergs PC, Scott G, Manavis J, Wainwright H, Simpson DA, McLean AJ (1994) Staining of amyloid precursor protein to study axonal damage in mild head injury. Lancet 344: 1055–1056.

Buki A, Siman R, Trojanowski JQ, Povlishock JT (1999) The role of calpain-mediated spectrin proteolysis in traumatically induced axonal injury. J Neuropathol Exp Neurol 58: 365–375.

Burnett MG, Detre JA, Greenberg JH (2005) Activation-flow coupling during graded cerebral ischemia. Brain Res 1047: 112–118.

Castejon OJ (1998) Electron microscopic analysis of cortical biopsies in patients with traumatic brain injuries and dysfunction of neurobehavioural system. J Submicrosc Cytol Pathol 30: 145–156.

Chen LJ, Wang YJ, Chen JR, Tseng GF (2015) NMDA receptor triggered molecular cascade underlies compression-induced rapid dendritic spine plasticity in cortical neurons. Exp Neurol 266: 86–98.

Chen JR, Wang YJ, Tseng GF (2003) The effect of epidural compression on cerebral cortex: a rat model. J Neurotrauma 20: 767–780.

Chen LJ, Wang YJ, Tseng GF (2010a) Compression alters kinase and phosphatase activity and tau and MAP2 phosphorylation transiently while inducing the fast adaptive dendritic remodeling of underlying cortical neurons. J Neurotrauma 27: 1657–1669.

Chen JR, Wang TJ, Wang YJ, Tseng GF (2010b) The immediate large-scale dendritic plasticity of cortical pyramidal neurons subjected to acute epidural compression. Neuroscience 167: 414–427.

Conti AC, Raghupathi R, Trojanowski JQ, McIntosh TK (1998) Experimental brain injury induces regionally distinct apoptosis during the acute and delayed post-traumatic period. J Neurosci 18: 5663–5672.

DeAngelis LM (2001) Brain tumors. N Engl J Med 344: 114–123.

de la Monte SM, Neely TR, Cannon J, Wands JR (2000) Oxidative stress and hypoxia-like injury cause Alzheimer-type molecular abnormalities in central nervous system neurons. Cell Mol Life Sci 57: 1471–1481.

Dobkin BH (1991) The rehabilitation of elderly stroke patients. Clin Geriatr Med 7: 507–523.

Ferezou I, Haiss F, Gentet LJ, Aronoff R, Weber B, Petersen CC (2007) Spatiotemporal dynamics of cortical sensorimotor integration in behaving mice. Neuron 56: 907–923.

Furuta T, Deschenes M, Kaneko T (2011) Anisotropic distribution of thalamocortical boutons in barrels. J Neurosci 31: 6432–6439.

Gallace A, Spence C (2009) The cognitive and neural correlates of tactile memory. Psychol Bull 135: 380–406.

Gao X, Chen J (2011) Mild traumatic brain injury results in extensive neuronal degeneration in the cerebral cortex. J Neuropathol Exp Neurol 70: 183–191.

Grossman KJ, Stein DG (2000) Does endogenous progesterone promote recovery of chronic sensorimotor deficits following contusion to the forelimb representation of the sensorimotor cortex? Behav Brain Res 116: 141–148.

Grünewald RA (1993) Ascorbic acid in the brain. Brain Res Brain Res Rev 18: 123–133.

Halpain S, Hipolito A, Saffer L (1998) Regulation of F-actin stability in dendritic spines by glutamate receptors and calcineurin. J Neurosci 18: 9835–9844.

Hayama T, Ogawa H (1997) Regional differences of callosal connections in the granular zones of the primary somatosensory cortex in rats. Brain Res Bull 43: 341–347.

Johansson RS, Cole KJ (1992) Sensory-motor coordination during grasping and manipulative actions. Curr Opin Neurobiol 2: 815–823.

Kao C, Forbes JA, Jermakowicz WJ, Sun DA, Davis B, Zhu J, Lagrange AH, Konrad PE (2012) Suppression of thalamocortical oscillations following traumatic brain injury in rats. J Neurosurg 117: 316–323.

Kharazia VN, Weinberg RJ (1994) Glutamate in thalamic fibers terminating in layer IV of primary sensory cortex. J Neurosci 14: 6021–6032.

Kundrotiene J, Wagner A, Liljequist S (2002) Extradural compression of sensorimotor cortex: a useful model for studies on ischemic brain damage and neuroprotection. J Neurotrauma 19: 69–84.

Kuypers NJ, Hoane MR (2010) Pyridoxine administration improves behavioral and anatomical outcome after unilateral contusion injury in the rat. J Neurotrauma 27: 1275–1282.

Lewen A, Hillered L (1998) Involvement of reactive oxygen species in membrane phospholipid breakdown and energy perturbation after traumatic brain injury in the rat. J Neurotrauma 15: 521–530.

Lin JL, Huang YH, Shen YC, Huang HC, Liu PH (2010) Ascorbic acid prevents blood-brain barrier disruption and sensory deficit caused by sustained compression of primary somatosensory cortex. J Cereb Blood Flow Metab 30: 1121–1136.

Marklund N, Clausen F, Lewander T, Hillered L (2001) Monitoring of reactive oxygen species production after traumatic brain injury in rats with microdialysis and the 4-hydroxybenzoic acid trapping method. J Neurotrauma 18: 1217–1227.

Martinez M, Brezun JM, Xerri C (2011) Sensorimotor experience influences recovery of forelimb abilities but not tissue loss after focal cortical compression in adult rats. PLoS One 6: e16726.

Matthews MA, Carey ME, Soblosky JS, Davidson JF, Tabor SL (1998) Focal brain injury and its effects on cerebral mantle, neurons, and fiber tracks. Brain Res 794: 1–18.

Mayer SA, Rincon F (2005) Treatment of intracerebral haemorrhage. Lancet Neurol 4: 662–672.

Mendez DR, Cherian L, Moore N, Arora T, Liu PK, Robertson CS (2004) Oxidative DNA lesions in a rodent model of traumatic brain injury. J Trauma 56: 1235–1240.

Moreira T, Cebers G, Salehi M, Wagner A, Liljequist S (2006) Impaired long-term habituation is dissociated from increased locomotor activity after sensorimotor cortex compression. Behav Brain Res 167: 9–22.

Noh KM, Koh JY (2000) Induction and activation by zinc of NADPH oxidase in cultured cortical neurons and astrocytes. J Neurosci 20: RC111.

Paolin A, Nardin L, Gaetani P, Rodriguez YBR, Pansarasa O, Marzatico F (2002) Oxidative damage after severe head injury and its relationship to neurological outcome. Neurosurgery 51: 949–954.

Paxinos G, Watson C (2007) The rat brain in stereotaxic coordinates. Academic Press, San Diego, California, USA.

Pettus EH, Povlishock JT (1996) Characterization of a distinct set of intra-axonal ultrastructural changes associated with traumatically induced alteration in axolemmal permeability. Brain Res 722: 1–11.

Posmantur RM, Kampfl A, Taft WC, Bhattacharjee M, Dixon CE, Bao J, Hayes RL (1996) Diminished microtubule-associated protein 2 (MAP2) immunoreactivity following cortical impact brain injury. J Neurotrauma 13: 125–137.

Posmantur RM, Newcomb JK, Kampfl A, Hayes RL (2000) Light and confocal microscopic studies of evolutionary changes in neurofilament proteins following cortical impact injury in the rat. Exp Neurol 161: 15–26.

Pratico D, Reiss P, Tang LX, Sung S, Rokach J, McIntosh TK (2002) Local and systemic increase in lipid peroxidation after moderate experimental traumatic brain injury. J Neurochem 80: 894–898.

Rice ME, Russo-Menna I (1998) Differential compartmentalization of brain ascorbate and glutathione between neurons and glia. Neuroscience 82: 1213–1223.

Rodriguez-Paez AC, Brunschwig JP, Bramlett HM (2005) Light and electron microscopic assessment of progressive atrophy following moderate traumatic brain injury in the rat. Acta Neuropathol 109: 603–616.

Saatman KE, Graham DI, McIntosh TK (1998) The neuronal cytoskeleton is at risk after mild and moderate brain injury. J Neurotrauma 15: 1047–1058.

Sanders MJ, Dietrich WD, Green EJ (2001) Behavioral, electrophysiological, and histopathological consequences of mild fluid-percussion injury in the rat. Brain Res 904: 141–144.

Sato M, Chang E, Igarashi T, Noble LJ (2001) Neuronal injury and loss after traumatic brain injury: time course and regional variability. Brain Res 917: 45–54.

Serrano F, Kolluri NS, Wientjes FB, Card JP, Klann E (2003) NADPH oxidase immunoreactivity in the mouse brain. Brain Res 988: 193–198.

Shimohama S, Tanino H, Kawakami N, Okamura N, Kodama H, Yamaguchi T, Hayakawa T, Nunomura A, Chiba S, Perry G, Smith MA, Fujimoto S (2000) Activation of NADPH oxidase in Alzheimer's disease brains. Biochem Biophys Res Commun 273: 5–9.

Tammariello SP, Quinn MT, Estus S (2000) NADPH oxidase contributes directly to oxidative stress and apoptosis in nerve growth factor-deprived sympathetic neurons. J Neurosci 20: RC53.

Turrigiano G (2012) Homeostatic synaptic plasticity: local and global mechanisms for stabilizing neuronal function. Cold Spring Harb Perspect Biol 4: a005736.

Tyurin VA, Tyurina YY, Borisenko GG, Sokolova TV, Ritov VB, Quinn PJ, Rose M, Kochanek P, Graham SH, Kagan VE (2000) Oxidative stress following traumatic brain injury in rats: quantitation of biomarkers and detection of free radical intermediates. J Neurochem 75: 2178–2189.

Vlachos A, Helias M, Becker D, Diesmann M, Deller T (2013) NMDA-receptor inhibition increases spine stability of denervated mouse dentate granule cells and accelerates spine density recovery following entorhinal denervation in vitro. Neurobiol Dis 59: 267–276.

Watanabe S, Hoffman JR, Craik RL, Hand PJ, Croul SE, Reivich M, Greenberg JH (2001) A new model of localized ischemia in rat somatosensory cortex produced by cortical compression. Stroke 32: 2615–2623.

Welker C, Woolsey TA (1974) Structure of layer IV in the somatosensory neocortex of the rat: description and comparison with the mouse. J Comp Neurol 158: 437–453.

Wilson MA, Johnston MV, Goldstein GW, Blue ME (2000) Neonatal lead exposure impairs development of rodent barrel field cortex. Proc Natl Acad Sci U S A 97: 5540–5545.

Winston CN, Chellappa D, Wilkins T, Barton DJ, Washington PM, Loane DJ, Zapple DN, Burns MP (2013) Controlled cortical impact results in an extensive loss of dendritic spines that is not mediated by injury-induced amyloid-beta accumulation. J Neurotrauma 30: 1966–1972.

Wu A, Ying Z, Gomez-Pinilla F (2006) Dietary curcumin counteracts the outcome of traumatic brain injury on oxidative stress, synaptic plasticity, and cognition. Exp Neurol 197: 309–317.

Yang H, Zhang X, Chopp M, Jiang F, Schallert T (2006) Local fluorouracil chemotherapy interferes with neural and behavioral recovery after brain tumor-like mass compression. Behav Brain Res 172: 80–89.

Zhang D, Dhillon HS, Mattson MP, Yurek DM, Prasad RM (1999) Immunohistochemical detection of the lipid peroxidation product 4-hydroxynonenal after experimental brain injury in the rat. Neurosci Lett 272: 57–61.

Zhang QG, Laird MD, Han D, Nguyen K, Scott E, Dong Y, Dhandapani KM, Brann DW (2012) Critical role of NADPH oxidase in neuronal oxidative damage and microglia activation following traumatic brain injury. PLoS One 7: e34504.

Zuo Y, Yang G, Kwon E, Gan WB (2005) Long-term sensory deprivation prevents dendritic spine loss in primary somatosensory cortex. Nature 436: 261–265.